Article

Thermal Design of Blackbody for On-Board Calibration of Spaceborne Infrared Imaging Sensor

Hye-In Kim [1], Bong-Geon Chae [2], Pil-Gyeong Choi [3], Mun-Shin Jo [3], Kyoung-Muk Lee [3] and Hyun-Ung Oh [1,2,*]

[1] Department of Smart Vehicle System Engineering, Chosun University, 375 Seosuk-dong, Dong-gu, Gwangju 501-759, Korea; khi130@chosun.kr
[2] STEP Lab Ltd., 40-37, Daehwa-dong, Daedeok-gu, Daejeon 306-020, Korea; bgchae@steplab.co.kr
[3] Mechatronics Groups, Hanwha Systems, 491-23, Gyeonggidong-ro, Namsa-myeon, Cheoin-gu, Yongin 272-210, Korea; pilgyeong123@hanwha.com (P.-G.C.); ms77.jo@hanwha.com (M.-S.J.); mook.lee@hanwha.com (K.-M.L.)
* Correspondence: ohu129@chosun.ac.kr

Abstract: In this study, we propose a thermal design for an on-board blackbody (BB) for spaceborne infrared (IR) sensor calibration. The main function of the on-board BB is to provide highly uniform and precise radiation temperature reference sources from 0 °C to 40 °C during the calibration of the IR sensor. To meet the functional requirements of BB, a BB thermal design using a heater to heat the BB during sensor calibration and heat pipes to transfer residual heat to the radiator after calibration is proposed and investigated both numerically and experimentally. The main features of the proposed thermal design are a symmetric temperature gradient on the BB surface with less than 1 K temperature uniformity, ease of temperature sensor implementation to estimate the representative surface temperature of the BB, a stable thermal interface between the heat pipes and BB, and a fail-safe function under one heat pipe failure. The thermal control performance of the BB is investigated via in-orbit thermal analysis, and its effectiveness is verified via a heat-up test of the BB under ambient conditions. These results indicate that the temperature gradient on the BB surface was obtained at less than 1 K, and the representative surface temperature could be estimated with an accuracy of 0.005 °C via the temperature sensor.

Keywords: infrared sensor; non-uniformity correction; blackbody; thermal design; fail-safe function; heat pipe

1. Introduction

Spaceborne infrared (IR) sensors are widely used in observation satellites to detect thermal IR radiation from an object, regardless of day- and nighttime constraints [1]. However, the IR sensor presents a non-uniformity characteristic owing to the time elapsed and repetitive on/off operation of the sensor in orbit. Consequently, this is one of the main factors causing the degradation of IR image quality. To obtain a high-quality IR image, the non-uniformity characteristic of the sensor should be periodically calibrated using an on-board blackbody (BB) system [2–7]. In addition, to increase the measurement accuracy of the IR sensor, two- or multi-point calibration using an on-board BB is required to provide various reference temperatures such that the gain and offset coefficients of the sensor can be calibrated in various calibration temperature ranges [8,9]. Therefore, to achieve high-quality images and increase the estimation accuracy of the IR sensor, an on-board BB system that can provide highly uniform and precise radiation sources at various temperature ranges is required.

To date, several types of on-board BB systems have been proposed and investigated [10–12]. Mason et al. [13] proposed an on-board BB calibration system, ATSR. It comprises two 140 mm-aperture BBs that can provide high and low reference temperatures of 30 and

−10 °C, respectively, for accurate remote sensing of sea surface temperatures. This performance was empirically demonstrated in the laboratory and in flight using long-term temperature readout tests, temperature uniformity measurements, and direct emissivity measurements. Olschewski et al. [14,15] proposed a BB system mounted on GLORIA for trace gas distributions. This system comprises two BBs that provide temperatures ranging from 10 K below to 30 K above ambient temperature, which is controlled by a thermo-electric cooler. The MODIS employed a high emissivity blackbody calibration source that operated from 170 K to 315 K. Xiong et al. [16,17] developed an Earth observing system Terra spacecraft, MODIS. It focuses on the application of the solar diffuser for the radiometric calibration of the sensor's reflective solar bands and the BB for radiometric calibration of its thermal emissive bands. The MODIS employed a high-emissivity blackbody calibration source that operated from 170 K to 315 K. Conventional BB systems are applied with multiple BBs, and each BB is controlled by a heater or TEC to provide various reference temperatures.

To overcome the disadvantages of the conventional BB system, such as its complexity and heft, Oh et al. [18,19] proposed a BB system for the on-board calibration of an imaging sensor that can provide a calibration temperature ranging from low to high temperatures using a single BB. This BB system comprises heaters that heat the BB from low to high temperatures during the calibration, a heat pipe to transfer residual heat on the BB immediately after calibration to the radiator on the spacecraft, and heaters on the radiator to maintain a certain temperature range of the BB during non-calibration. In this study, it was reported that a BB with a vertically installed heat pipe provides a better circular symmetric temperature distribution with a smaller temperature gradient on the BB surface, and that it can effectively and easily estimate the representative surface temperature of the BB based on a few embedded temperature sensors. A thermal paste or adhesive is applied to integrate the heat pipe into the BB. This design is sensitive to mechanical loadings induced by thermal deformation, launch vibration, and misalignment; consequently, the BB demonstrates performance variation owing to the change in the thermal contact coefficient on the thermal interface between the heat pipe and BB. Furthermore, the criticality of the system results in complete system failure, and the system is devoid of a fail-safe function to avoid the single point failure of the heat pipe.

In this paper, we propose an on-board BB system with the same functionality and performance as the conventional system [18,19]. The proposed BB system is developed for an Earth observation IR imaging sensor, and IR sensor calibration is performed in a temperature range from 0 to 40 °C, according to the observed temperature of the IR sensor. The BB system can overcome the aforementioned drawbacks, such as mechanical loadings that are sensitive to the heat pipe thermal interface and the lack of a fail-safe function. The design concept of the proposed BB system is to provide a flange-type mechanical interface, in which the heat pipe is mechanically clamped to the BB to guarantee a stable thermal conductivity under launch vibration and in-orbit thermal environments. Furthermore, it allows an easier integration of the dual heat pipes to prevent the single-point failure of the heat pipe. Furthermore, the temperature sensors used to measure the representative surface temperature on the BB are directly attached to the rear side of the BB, unlike embedded temperature sensors applied to the conventional BB, which guarantees easier workmanship. The BB calibration concept was used to heat the BB to the target temperature and perform sensor calibration using a uniform and precise radiation temperature source during the cooling phase of the BB. The feasibility of the newly proposed design was validated through an in-orbit thermal analysis. In addition, a BB heat-up test under ambient conditions was performed to evaluate the BB system. The analysis and test results show that the proposed on-board BB system was successfully designed and validated to meet the requirements.

2. Thermal Design of On-Board BB

The BB system proposed in this paper can provide various radiation temperatures for the on-board calibration of spaceborne IR sensors. Figure 1 illustrates the on-board

calibration process using the BB and a tilt-mirror mechanism [20]. The tilt mirror is designed to have a high reflectance of 99% to accurately reflect the radiation temperature from the BB to reflector. To calibrate the IR sensor, the tilt mirror was periodically deployed to reflect the referenced radiation temperature from the BB and then re-stowed after calibration.

The BB system primarily aims to provide a highly uniform radiation temperature when it is in alignment with the tilt mirror. Furthermore, the main requirements for the BB thermal design were to provide a radiance temperature of approximately 40 °C within 500 s and temperature uniformity under 1 K on the BB surface during the calibration phase. Furthermore, the BB should be cooled from 40 °C to 0 °C within 10,800 s after BB heat-up for periodic sensor calibration in two orbits.
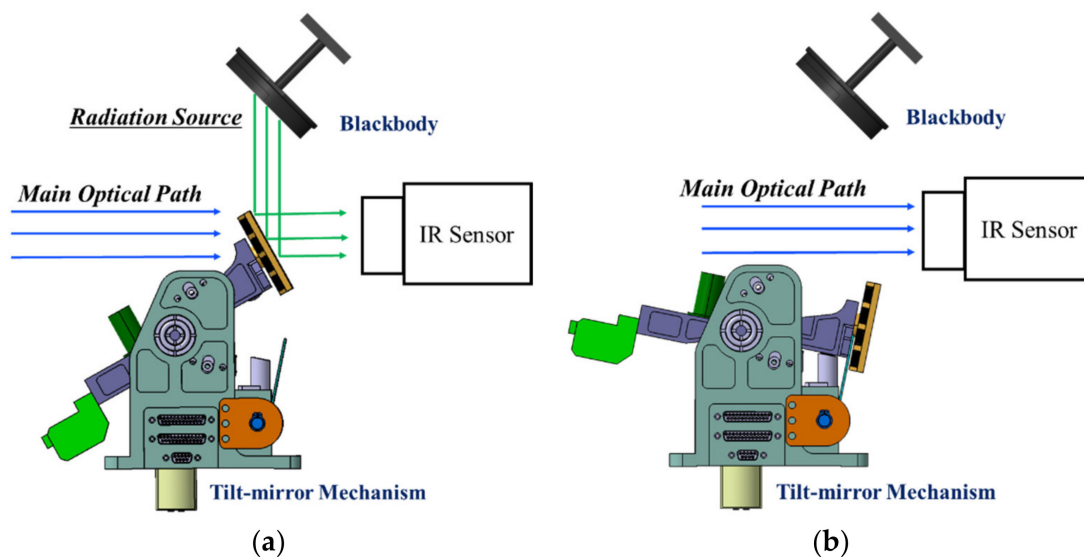
Figure 1. On-board calibration concept using BB and tilt-mirror (**a**) Imaging mode; (**b**) calibration mode.

Figure 2a shows the mechanical configuration of the on-board BB system proposed in this study. To meet this requirement, a highly reliable and accurate thermal design is required. The BB system comprises heaters on the rear side of the BB to enable heating up to 40 °C and heat pipes to transfer residual heat on the BB surface to the radiator on the spacecraft (S/C) to provide a radiation temperature source during the cooling down of the BB. Additionally, the heaters were applied to the radiator to maintain the BB surface temperature at 20 °C during the non-calibration range. The radiator heater was controlled using a thermostat with the required temperature set points to simplify the system. The V-groove shape was implemented on the BB front side to obtain a higher emissivity than the flat surface. A cylindrical baffle was implemented to obstruct thermal noise from other heat sources. In addition, thermal washers were used to realize conductive decoupling between the radiator and S/C. Furthermore, the rear side of the BB and radiator were covered with a multilayer insulator (MLI) for radiation decoupling. Heat pipes with a diameter of 9 mm were applied, and the specifications of the heat pipe are presented in Table 1. The heat pipe enables per-orbit calibration to be performed prior to imaging by transferring the residual heat of the BB after heating; this is beneficial as approximately 30 min is required to cool down the BB to approximately 0 °C. In addition, a bent-shaped heat pipe was adopted to mitigate the forces transmitted to the BB induced by launch vibration and thermal deformation in in-orbit conditions. The heat pipe was clamped to the mechanical flange on the BB, as shown in Figure 2b, to guarantee a stable thermal conductivity without any alignment shift and thermal deformation under launch vibration and in-orbit thermal environments. This interface allows the easier integration of the dual heat pipes to prevent the single-point failure of the heat pipe. Furthermore, the heat pipe flange interface enables a circular symmetric temperature distribution to be obtained on the BB surface, which renders it easier to estimate the representative surface temperature

from the temperature sensors. To improve the thermal conductivity between the BB and heat pipe, a high thermal conductivity Cho-Therm was applied to the flange interface. Four temperature sensors were attached directly to the rear side of the BB, i.e., two at the primary and two at the redundant, to estimate the reference surface temperature of the BB. It guarantees easier workmanship, unlike the embedded temperature sensor applied to conventional BB. Furthermore, the proposed BB is mounted inside the spacecraft, and the total ionizing dose (TID) level under the in-orbit environment is approximately 2 Krad. The temperature sensor and heater installed on the BB are space-grade products with a TID level of 100 Krad, which is higher than the predicted TID. Furthermore, the surface coating and MLI also have a space heritage; hence, the proposed blackbody system ensures proper operation throughout its mission lifetime.

Figure 3 shows an example of the operating principle of an on-board BB for IR sensor calibration. The temperature of the BB was maintained at 20 °C in the non-calibration region using a radiator heater to minimize the thermal noise effect from the BB to the optics with a view factor to the BB, as well as to perform the calibration as necessitated. In this region, the tilt-mirror mechanism is stowed to acquire the main optical path. For the calibration of the IR sensor, the BB was heated to approximately 40 °C, and the sensor was calibrated in the cooling region of the BB surface from 40 °C to 0 °C to provide various referenced radiance temperature sources, where the tilt mirror maintains the deployed configuration to reflect the radiance temperature from the BB to the sensor. The BB was re-heated to 20 °C using the radiator heater after the BB was cooled down to 0 °C, and the tilt mirror was re-stowed.
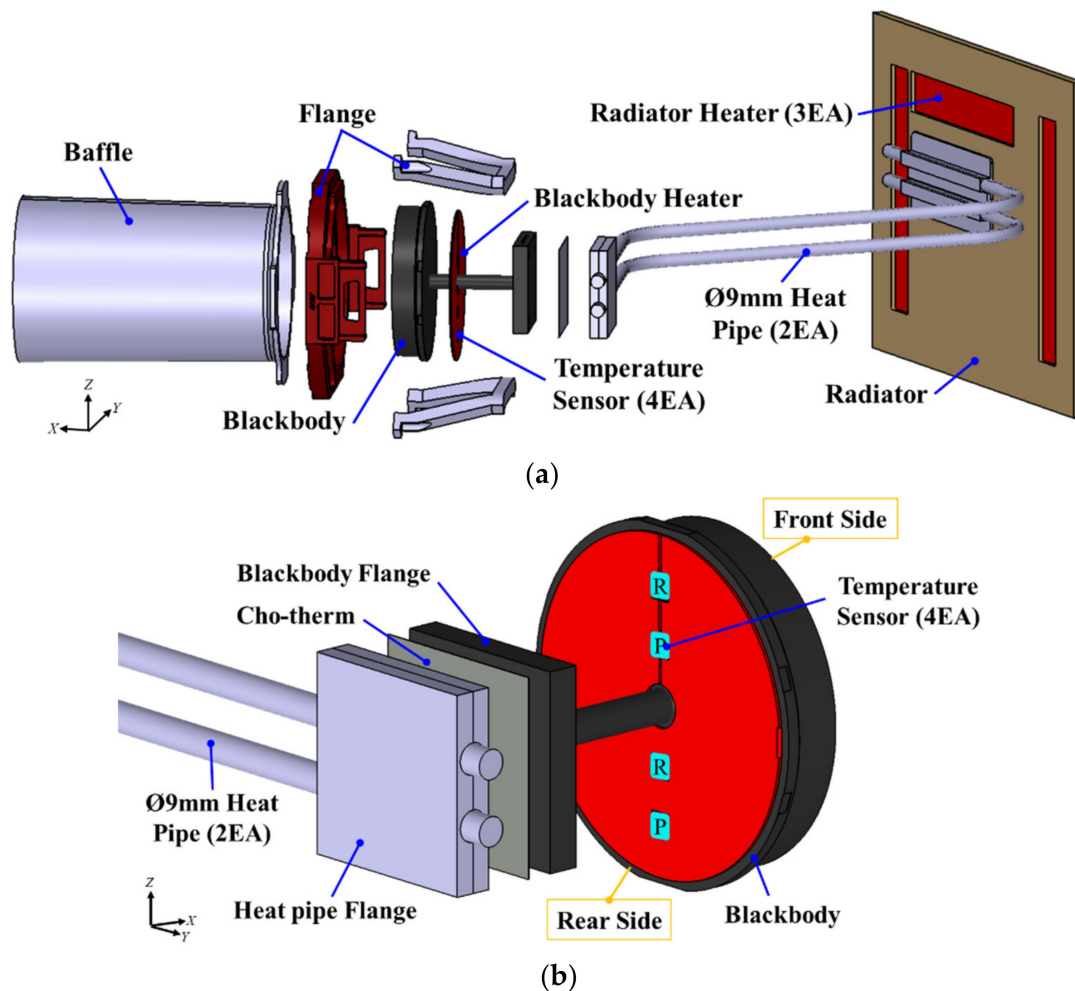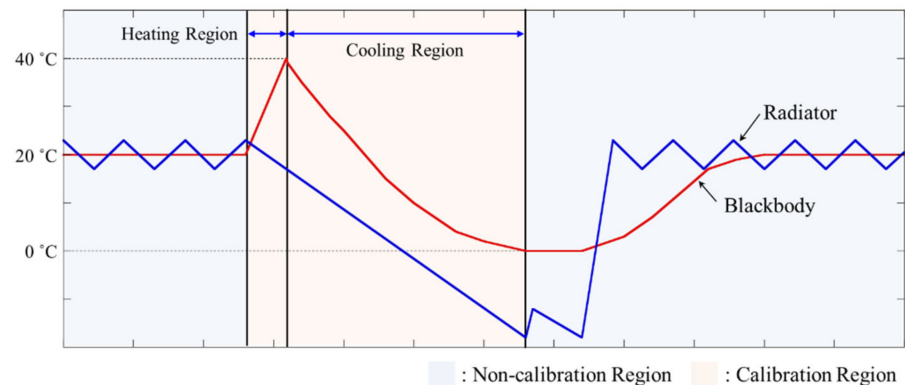

(a)

(b)

Figure 2. Mechanical configuration of BB. (**a**) Overall view; (**b**) detailed view.

Table 1. Specifications of 9 mm heat pipe.

| Specifications	9 mm Heat Pipe
Material	Al6063
Working Fluid	NH3
Outer Diameter	9 mm
Inner Diameter	6.7 mm
Evaporator Length	50 mm
Condenser Length	80 mm

Figure 3. Operating concept of on-board BB.

3. In-Orbit Thermal Analysis of On-Board BB

3.1. Thermal Mathematical Model

To confirm the effectiveness of the thermal design of the on-board BB, an in-orbit thermal analysis was performed. Figure 4 shows the thermal mathematical model (TMM) of the BB. To investigate the thermal behavior of the BB during its in-orbit operation, the TMM of the BB was integrated with the simplified TMM of the spacecraft with solar panels, as shown in Figure 4b. The total number of nodes used in the TMM was 746, the conductor for constructing thermal networks was 11, and the heat load for simulating the heater was 2. In this study, the TMM was constructed in Thermal Desktop [21], which is a CAD-based geometric interface, and the thermal analysis was performed using SINDA/FLUINT and RadCAD [22].

The heater power and temperature set points for the radiator heater control are summarized in Table 2. Table 3 shows the material and thermo-optical properties used in the thermal analysis. Table 3 shows the calculated contact conductance values used in the thermal analysis. To simplify the TMM, conductors with a value of 2.294 W/K (calculated from the specifications of the heat pipes shown in Table 4) were applied as the thermal chain between the BB and radiator. The orbital conditions and in-orbit profile in the worst hot and cold cases applied in the analysis are shown in Table 5 and Figure 5, respectively. For the analysis, we assumed that the orbit was a sun-synchronous orbit with an altitude of 561 km, and that it had an eclipse region of 30 min per orbit. The front side of the S/C with an optical telescope maintained anti-sun pointing in the non-imaging region for solar power generation from the solar panels. The S/C maintained nadir, pointing at the eclipse region to warm up the telescope via the Earth's IR light and albedo. The boundary temperature of the BB used in the analysis was set to 25 °C and 15 °C, which corresponds to the boundary temperature of S/C in the worst hot and cold cases, respectively.

(**a**)

(**b**)
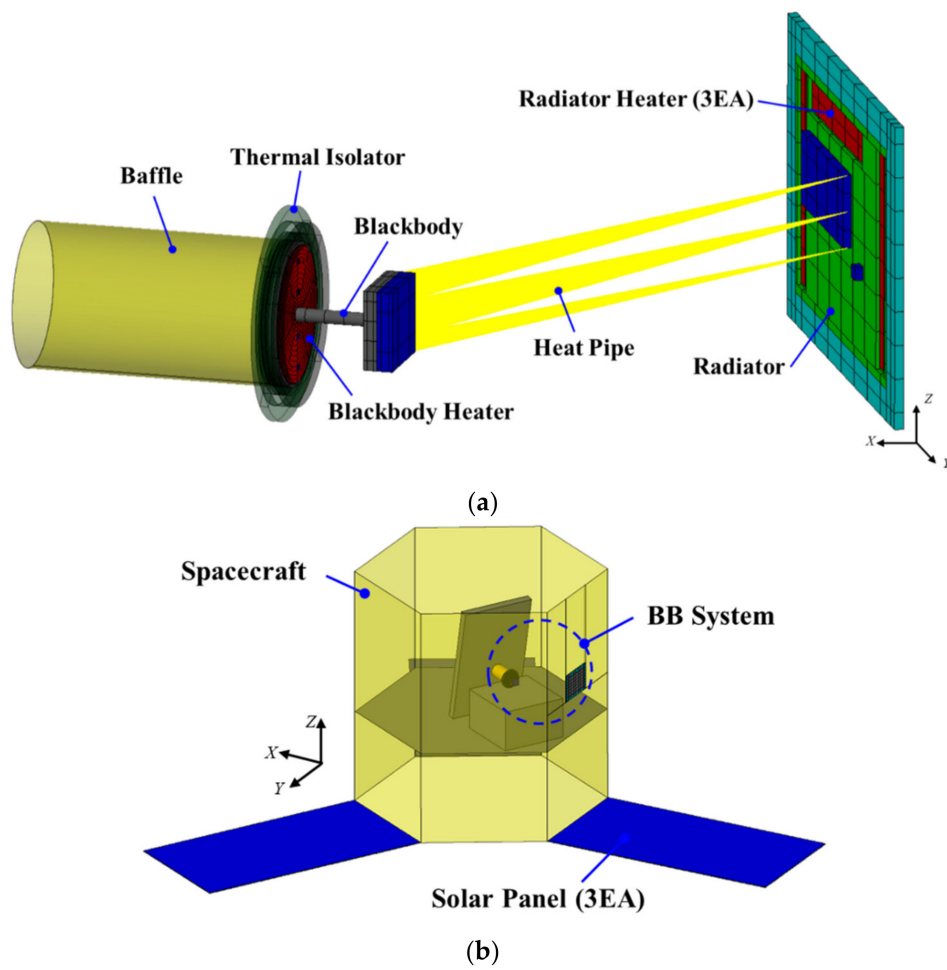
Figure 4. Thermal mathematical model of BB system for in-orbit analysis. (**a**) Detailed view; (**b**) Overall view.

Table 2. Heat dissipation and on/off set-point of heaters.

Item	Total Heat Dissipation (W)	On/Off Set-Point (°C)	Remark
BB Heater	40.83	—	—
Radiator Heater	30 (3EA)	17/23 −18/−12	Non-calibration Region Calibration Region

Table 3. Material and thermo–optical properties.

Material Properties			
Material	Conductivity (W/m/K)	Density (kg/m³)	Specific Heat (J/kg/K)	Remark
Al-6063	200	2768	879.2	BB, radiator
Al-6061	170	2768	879.2	Baffle
Heater	0.12	1410	1090	Heater
G10	0.288	1850	1400	Thermal isolator
Ti-6Al-4V	17	4430	1590	Flange

Table 3. *Cont.*

Thermo-Optical Properties				
Material	Solar Absorptivity (α)	IR Emissivity (ε)	α/ε	Remark
Acktar black coating	0.98	0.98	1	BB (front side)
MLI	0.05	0.05	1	BB (rear side), heat pipe, radiator (internal)
OSR	0.24	0.80	0.3	Radiator (external)
White paint	0.70	0.90	0.78	Solar panel (rear side)

Table 4. Summary of contactor value.

Component		Value	Remark
From	To		
BB Flange	Radiator flange	2.294 W/K	Heat pipe normal operation
		1.2 W/K	One heat pipe failure
Blackbody	Thermal isolator	48 W/m^2/K	Thermal washer
Thermal isolator	Baffle	48 W/m^2/K	Thermal washer
Blackbody heater	Blackbody	2000 W/m^2/K	Coupling
Radiator heater	Radiator	2000 W/m^2/K	Coupling

Table 5. Orbit parameter of BB.

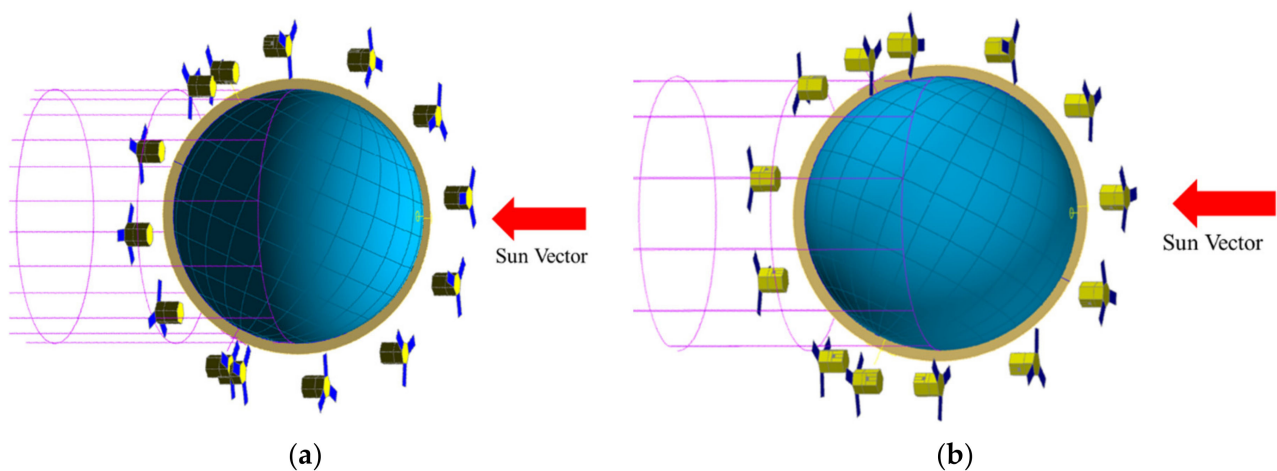| Parameter	Orbit Condition	
	Worst Hot	Worst Cold
Orbit Type	Sun Synchronous Orbit	
Period (min)	95.88	
Solar flux (W/m^2)	1420	1284
Albedo coefficient	0.35	0.3
IR flux (W/m^2)	249	227
Boundary condition (°C)	25	15

(a)　　　**(b)**

Figure 5. In-orbit profile of BB. (**a**) Worst hot case; (**b**) worst cold case.

3.2. In-Orbit Thermal Analysis Results

To verify the feasibility of the thermal design of the proposed BB system, we performed an in-orbit thermal analysis using the TMM, as shown in Figure 4, under the proposed orbit information and boundary condition of S/C.

Figure 6 shows an example of the temperature profile of the BB surface and radiator under the worst hot and cold normal operating conditions, respectively. The results show that the BB is maintained at approximately 20 °C by the radiator heater during the non-calibration region and was heated from 20 °C to 40 °C in the heating range of the BB within 224 s (hot case) and 230 s (cold case). In addition, 5793 s (hot case) and 5721 s (cold case) were required to cool the BB surface to 0 °C after the BB was heated; the abovementioned time durations correspond to those required for the on-board calibration to provide various radiance temperatures for the sensor calibration. The BB was re-heated to 20 °C after the sensor calibration was completed. This indicates that the sensor calibration can be performed periodically because the cooling time was less than 10,800 s. Furthermore, the heater power dissipation was optimized to satisfy the thermal design requirement of the BB. In addition, it was confirmed that the radiator heater duty was 44.78% and 44.74% in the worst hot and cold cases, respectively.
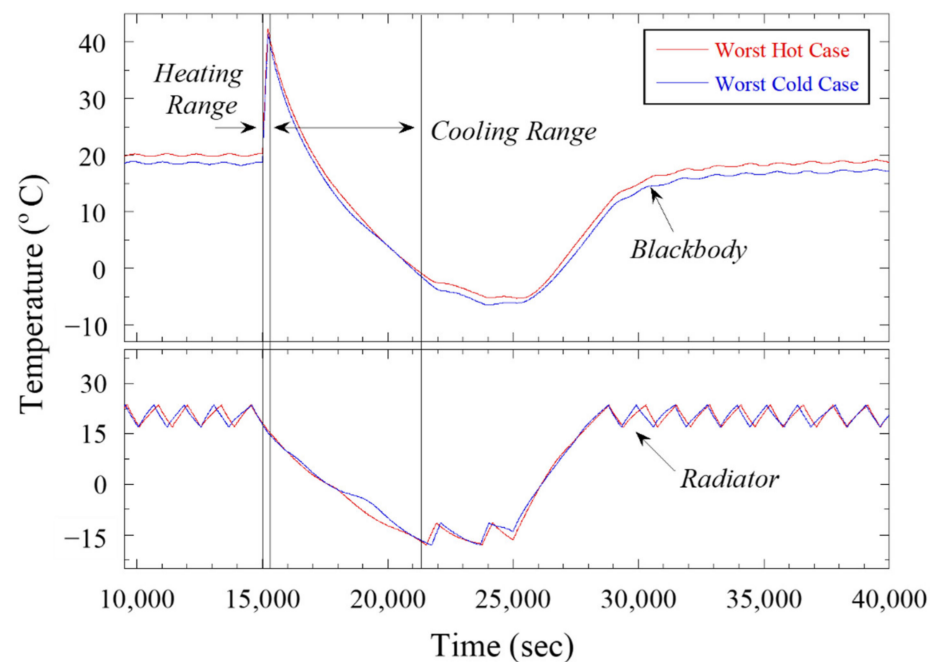
Figure 6. Temperature profile on BB surface and radiator in normal heat pipe operation conditions.

Figures 7 and 8 show the temperature contour maps of the BB surface at a specific time in the heating and cooling ranges, respectively. Figure 7, obtained from the heating range, shows an asymmetric temperature distribution even though the temperature gradient ΔT on the BB surface was less than the requirement of 1 °C. However, the temperature contour maps obtained at the cooling region show a circular symmetric temperature distribution on the BB surface, which is inconsistent with the heating range of the BB as shown in Figure 8. This indicates that the representative surface temperature of the BB can be estimated more easily and accurately by applying a weighting factor to the limited number of temperature sensors positioned on the rear side of the BB. The maximum value of ΔT on the BB surface in the cooling region was 0.25 °C when the average temperature of the BB surface reached approximately 40 °C. This indicates that the proposed BB system was successfully designed to achieve the required design objectives.
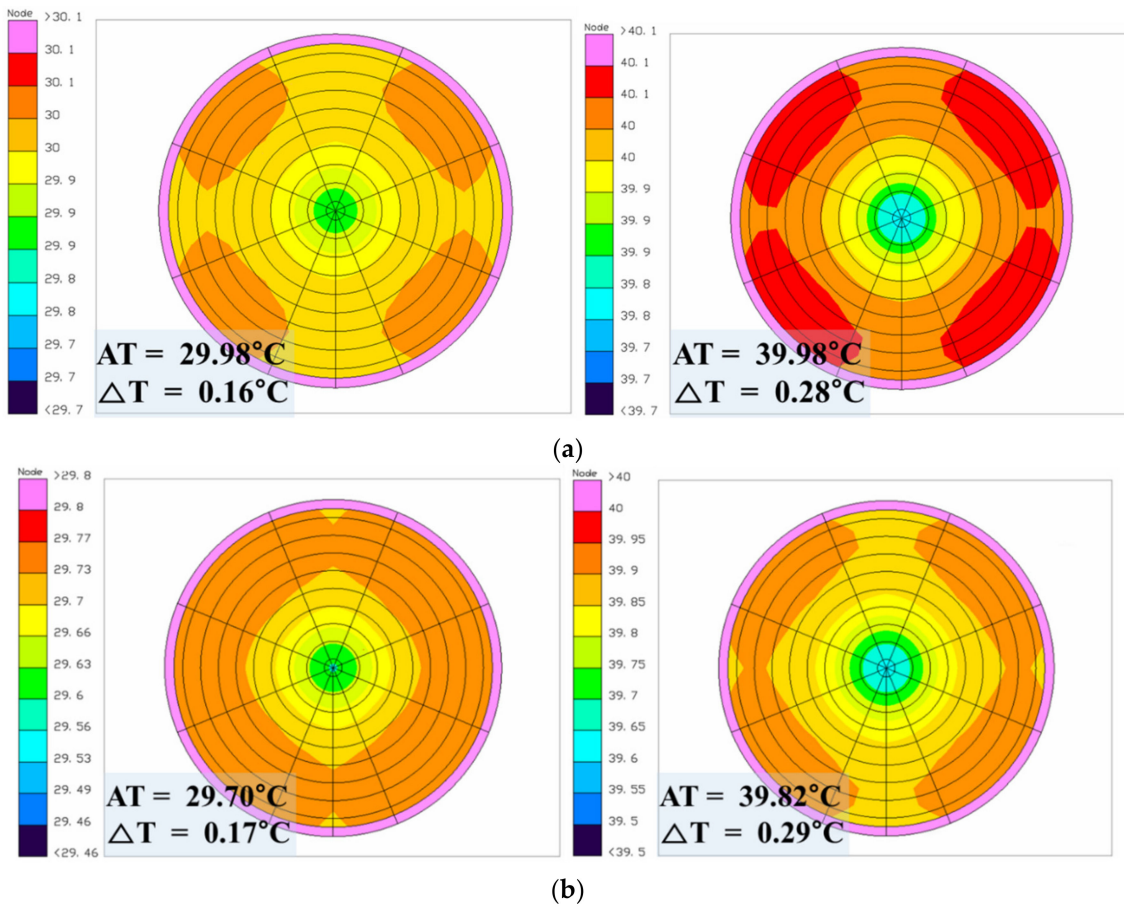
Figure 7. Temperature distribution on BB surface in heating range at heat pipe normal operation condition. (**a**) Worst hot case; (**b**) worst cold case; AT: average temperature of BB surface; ΔT: temperature gradient on BB surface.
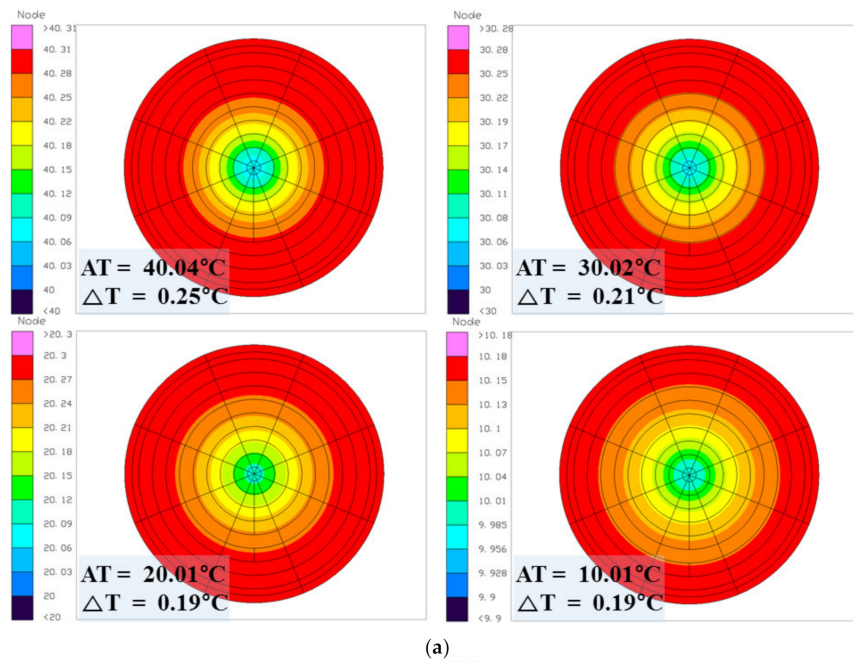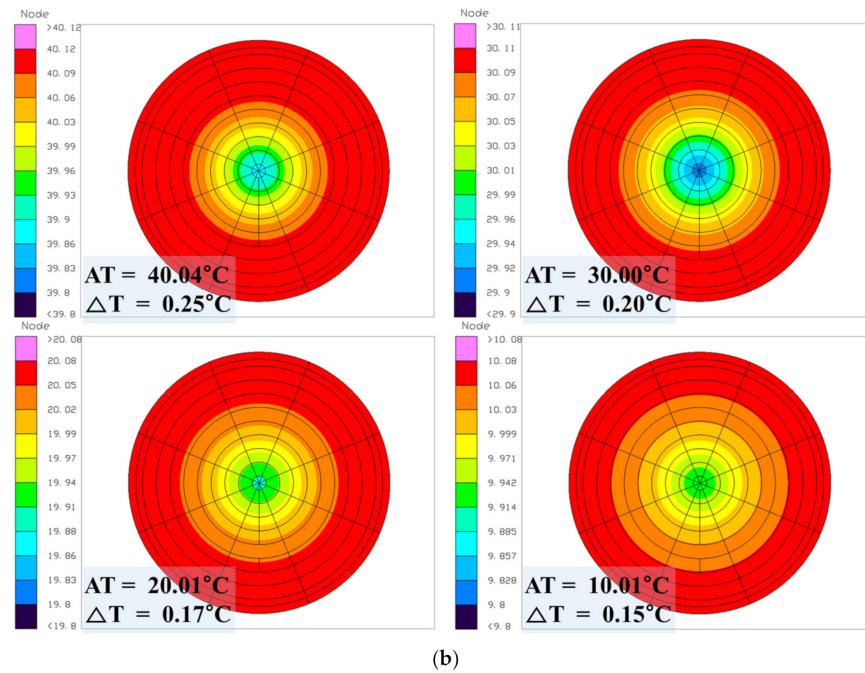

Figure 8. *Cont.*

(**b**)

Figure 8. Temperature distribution on BB surface in cooling range at heat pipe normal operation condition. (**a**) Worst hot case; (**b**) worst cold case; AT: average temperature of BB surface; ΔT: temperature gradient on BB surface.

To verify the fail-safe design of the heat pipe, one heat pipe failure case was analyzed. Figure 9 illustrates the temperature profile of the BB surface and radiator with one heat pipe failure case in the worst hot case. In addition, the figure shows a comparison of the results obtained from the normal operation case. In this analysis, the thermal conductance during heat pipe normal operation is 2.294 W/K. Furthermore, thermal conductance in the case of a single heat pipe failure is 1.2 W/K as the residual heat is also transferred through the external wick structure of the failed heat pipe. Nevertheless, the BB surface cooling time in one heat pipe failure case was 6138 s, which differed by only 345 s, compared with that of the heat pipe's normal operation condition. Furthermore, Figure 10 illustrates the temperature contour on the BB surface with one heat pipe failure in the worst hot case. The maximum value of ΔT on the BB surface in the cooling region is 0.24 °C when the average temperature of the BB surface reaches approximately 40 °C. The temperature gradient on the BB surface is obtained in circular symmetric distribution, which is similar to the normal operating condition because the residual heat is dissipated through the mechanical flange on the BB. This indicates that even if one heat pipe fails, it can satisfy all the requirements and reliably maintain the performance of the BB system.

The representative surface temperature of the BB should be estimated precisely from temperature sensors for the calibration of the image sensor. To estimate the BB surface temperature more accurately using temperature sensors, we used the following first-order equation:

$$T_E = (W_1 \times T_1) + (W_2 \times T_2) + W_3 \tag{1}$$

where T_E is the surface temperature from the first-order equation, and T_1 and T_2 are the temperatures obtained from the temperature sensors shown in Figure 11. W_1, W_2, and W_3 are calculated numerically using the least-squares method, as follows:

$$J(W_1, W_2, W_3) \equiv \sum_{i=1}^{n}(T_{Ai} - T_{Ei})^2 \tag{2}$$

where n is the total amount of predicted average temperature data for the estimation, and T_A is the average temperature on the BB surface.
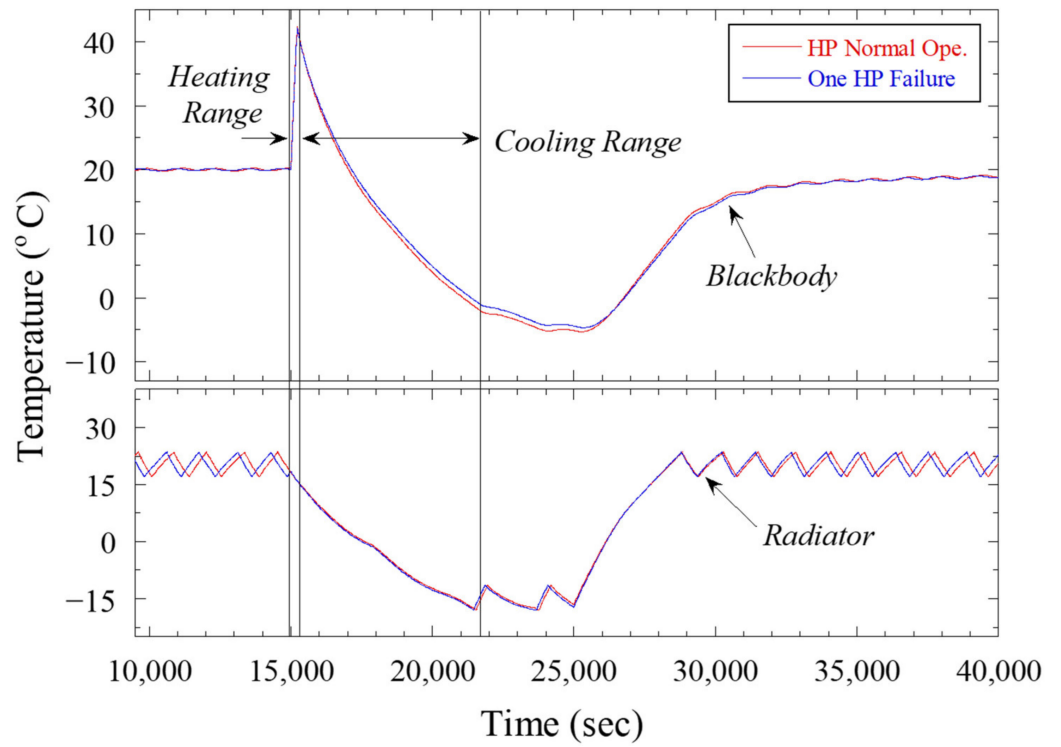
Figure 9. Temperature profile on BB surface and radiator with one heat pipe failure case in the worst hot case.
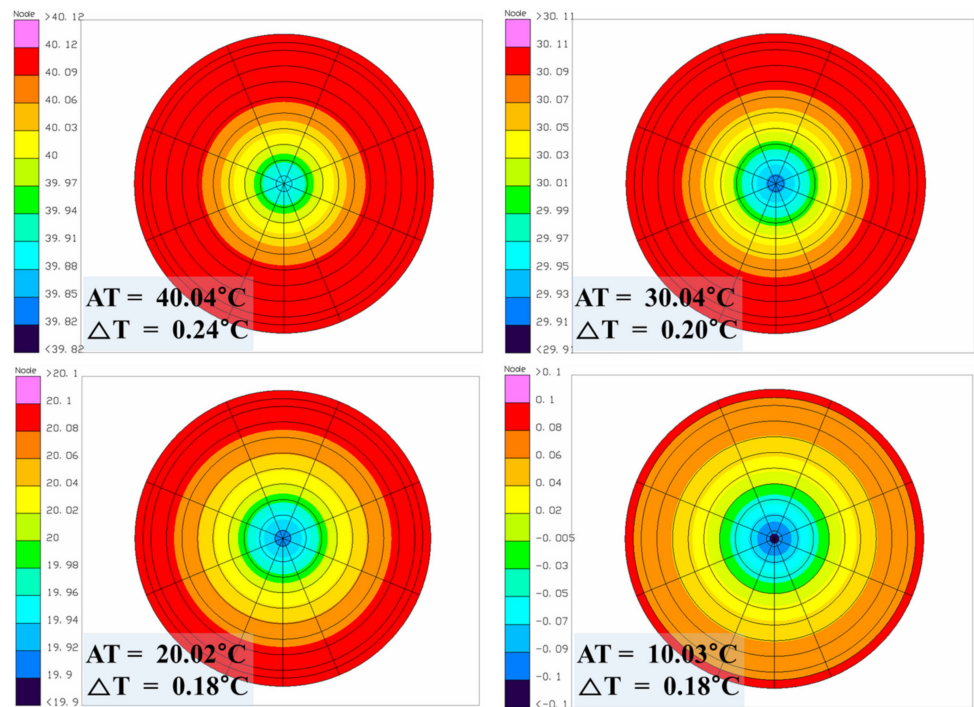
Figure 10. Temperature distribution on BB surface in cooling range at one heat pipe failure condition in the worst hot case; AT: average temperature of BB surface; ΔT: temperature gradient on BB surface.
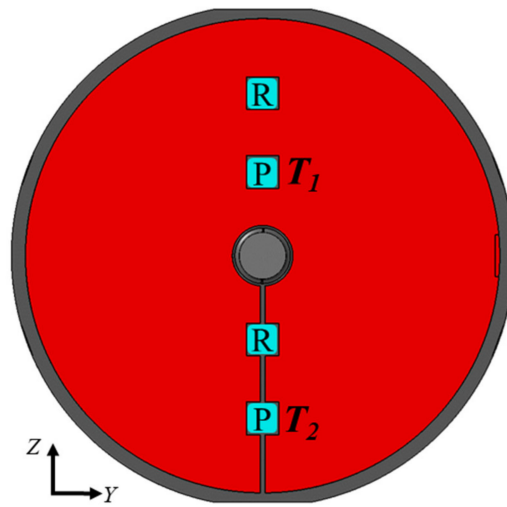
Figure 11. Position of temperature sensors.

Figure 12 shows a comparison of the estimation accuracy of T_A–T_E in the worst hot and cold cases with respect to the heating and cooling regions. The maximum value of estimation accuracy obtained from the heating region from 20 °C to 40 °C was 0.03 °C, which is higher than that obtained from the cooling region owing to its asymmetric temperature gradient characteristics, as shown in Figure 6. However, the results obtained from the cooling region can be used to estimate the representative surface temperature of the BB precisely to an accuracy of less than 0.005 °C, even under the worst condition where the BB heater was turned off immediately after reaching 40 °C. This indicates that the thermal design concept of the BB, which allows a circular symmetric temperature gradient to be obtained at the cooling region, is feasible for estimating a representative surface temperature of the BB with high accuracy by applying a weighting factor to the output values of the temperature sensors.
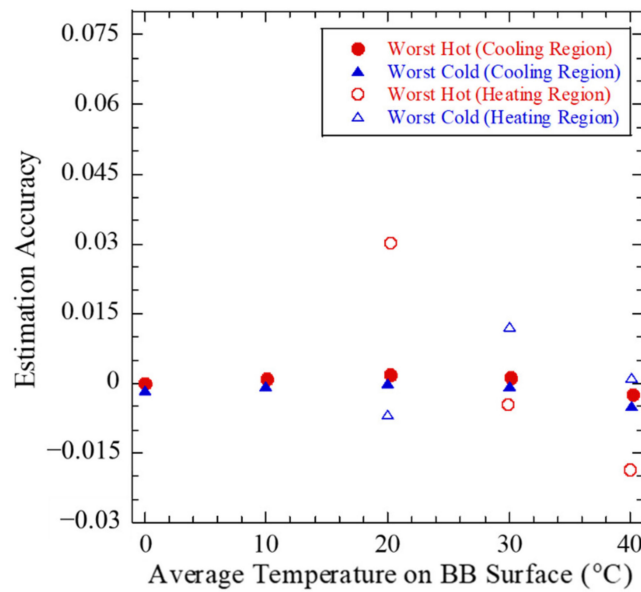

Figure 12. Estimation accuracy of BB.

The results of the above in-orbit thermal analysis are summarized in Table 6. These results demonstrate that even if a single heat pipe is damaged, it is possible to satisfy all design requirements without much difference in normal operation. Therefore, the proposed

BB system's thermal design demonstrated that the heat pipe fail-safe function could be realized in in-orbit thermal environments.

Table 6. Summary of thermal analysis results.

Worst Hot	Heat Pipe Normal Operation		One Heat Pipe Failure		Remark
	Worst Hot	Worst Cold	Worst Hot	Worst Cold	
Heating time (s)	224	230	224	230	<500
Maximum temperature on BB surface (°C)	42.46	41.38	42.18	41.15	>40
Cooling time (s)	5793	5721	6138	6033	<10,800
Maximum ΔT in cooling range (°C)	0.25	0.25	0.24	0.23	<1
Estimation accuracy (°C)	0.0025	0.0049	-	-	-
Radiator heater duty cycle (%)	44.78	44.74	40.86	40.83	<80

4. BB Heat-Up Test Results

To verify the performance of the BB prior to testing under vacuum conditions, we performed a BB function test under ambient conditions. Figure 13 shows the configuration of the BB function test setup under ambient conditions. It comprises an IR camera to measure the BB surface temperature and a cold plate to transfer the residual heat of the BB after heating. The test configuration was the same as the thermal design configuration, as shown in Figure 2, except for the radiator, which was simulated by the cold plate combined with a circular bath. The BB function test was performed when the environmental temperature of the thermal chamber was set to 20 °C and 0 °C. The heat-up test was performed at 20 °C to verify the BB heat-up time and BB surface temperature distribution in the calibration region. In addition, the cooling time and temperature distribution of the BB surface were measured at an ambient temperature of 0 °C.
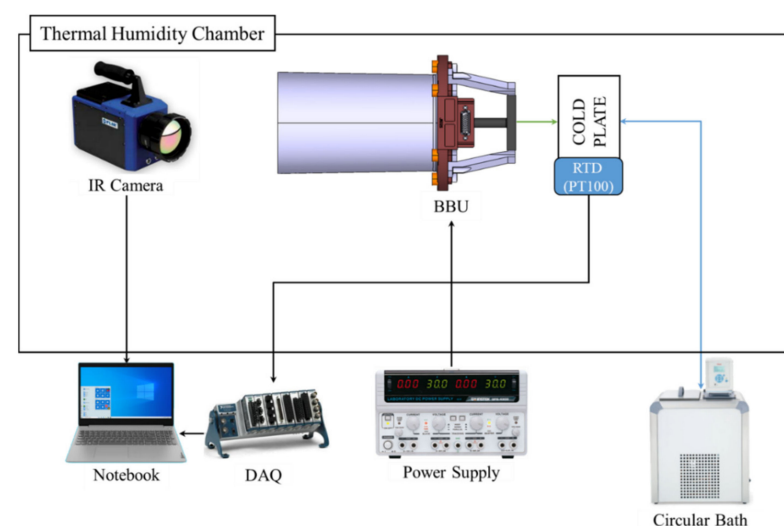
Figure 13. BB heat-up test setup in ambient condition.

Figure 14 shows the temperature profile of the BB surface and the cold plate temperature measured using the temperature sensor during the BB heat-up test. The test results indicate that the BB surface temperature increased from 20 °C to 45.03 °C within 208 s. In addition, 3510 s was required to cool the BB surface to 0 °C after the BB was heated, which is consistent with the on-board calibration range for providing various radiance temperatures.

Figure 15 shows the temperature distribution on the BB surface measured using an IR camera when the temperature reached approximately 40 °C, 30 °C, 20 °C, 10 °C, and 0 °C during the BB heat-up test at an ambient temperature of 0 °C. The maximum temperature difference recorded on the BB surface was 0.83 °C at an average surface temperature of 40 °C. This value satisfies the maximum temperature gradient requirement of less than 1 °C on the BB surface, although the value was measured under ambient conditions. Furthermore, the figure shows that the top side of the BB surface was hotter than the bottom side, and it was speculated that convective heat transfer on the bottom side was more active than that on the top side. However, a better BB performance can be expected under vacuum conditions because the convection effect is negligible. These function test results indicate that the proposed BB design is effective for satisfying the required function and performance of on-board BB.
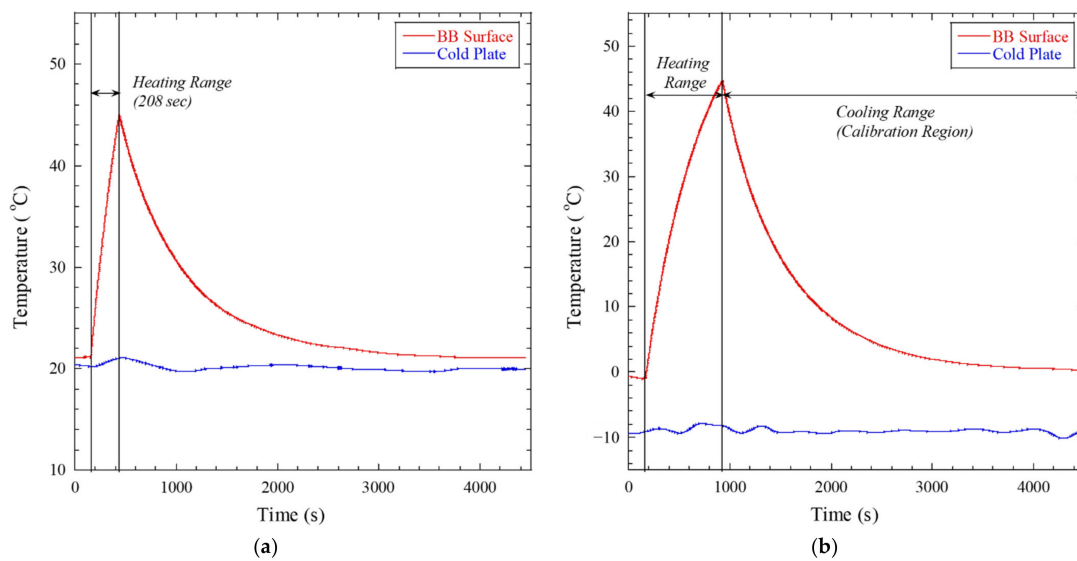

Figure 14. Temperature profile on BB surface measured using temperature sensors: (**a**) 20 °C boundary condition; (**b**) 0 °C boundary condition.
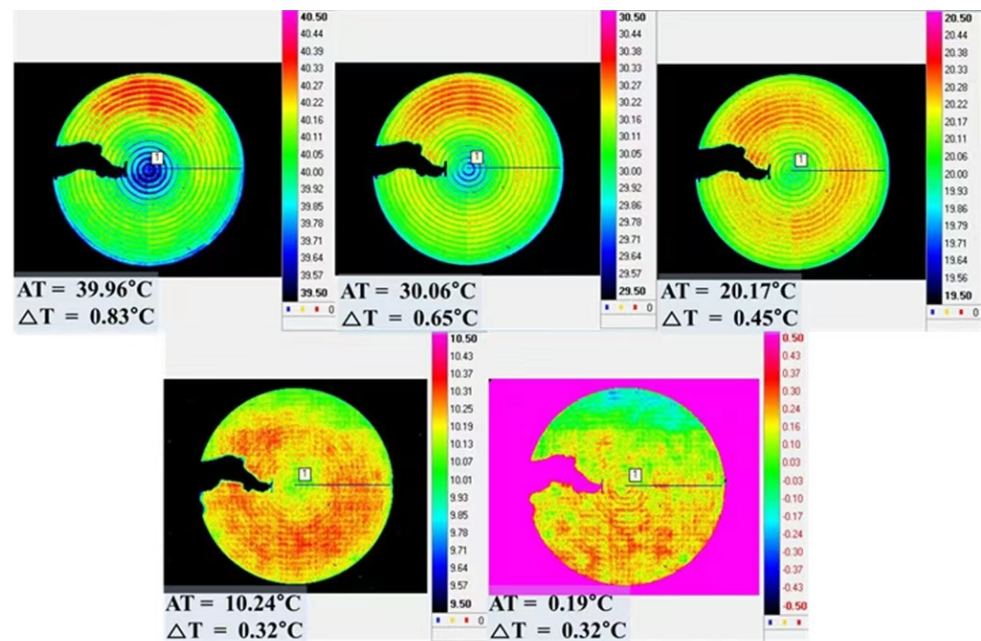

Figure 15. Temperature distribution on BB surface measured using IR camera; AT: average temperature of BB surface; ∆T: temperature gradient on BB surface.

5. Discussion and Conclusions

In this study, an on-board BB system for calibrating a spaceborne IR sensor with a fail-safe function in the case of one heat pipe failure was proposed, to overcome the conventional on-board BB calibration system. To obtain the fail-safe function of heat pipe, the two heat pipes were clamped to the mechanical flange interface to guarantee a stable thermal distribution to be obtained on the BB surface. The BB system primarily aims to provide a highly uniform and precisely known radiation temperature when performing image sensor calibration. The feasibility and characteristics of the temperature uniformity of the BB during the calibration were numerically investigated via an in-orbit thermal analysis. The analysis results reveal that the temperature gradient on the BB surface was obtained at less than 1 K, and the BB surface was cooled from 40 to 0 °C within two orbits. In addition, representative surface temperature could be estimated with an accuracy of 0.005 °C. Furthermore, to validate the heat pipe fail-safe function, one heat pipe failure case was analyzed. This result indicates that the thermal behavior is similar to that of the normal operating condition of the heat pipe because the residual heat is dissipated through the mechanical flange on the BB. These results indicate that the residual heat from the BB can be sufficiently transported through one heat pipe. Therefore, the flange-type mechanical interface effectively prevented the single-point failure of the heat pipe without compromising performance.

In addition, a heat-up test under ambient conditions was performed to verify the effectiveness of the BB design. It is considered that the convection effect inside the humidity chamber is more active on the bottom side of the BB, and this is the main cause of increasing the temperature gradient on the BB surface. Nonetheless, it is possible to satisfy all requirements arising from the blackbody surface. The overall test results indicate that the thermal design proposed in this study successfully achieved the design goals of the on-board BB system.

References

1. Khare, S.; Singh, M.; Kaushik, B.K. Real time non-uniformity correction algorithm and implementation in reconfigurable architecture for infrared imaging systems. *Def. Sci. J.* **2019**, *69*, 179–184. [CrossRef]
2. Çalık, R.C.; Tunali, E.; Ercan, B.; Oz, S. A Study on Calibration Methods for Infrared Focal Plane Array Cameras. *VISIGRAPP* **2018**, *4*, 219–226. [CrossRef]
3. Sheng, M.; Xie, J.; Fu, Z. Calibration-based NUC Method in Real-time Based on IRFPA. *Phys. Procedia* **2011**, *22*, 372–380. [CrossRef]
4. Lau, A.S. The Narcissus Effect in Infrared Optical Scanning Systems. In *Stray Light Problems in Optical Systems*; International Society for Optics and Photonics: Bellingham, WA, USA, 1977; Volume 107, pp. 57–63. [CrossRef]
5. Mudau, A.; Willers, C.J.; Griffith, D.; le Roux, F.P.J. Non-uniformity correction and bad pixel replacement on LWIR and MWIR images. In Proceedings of the 2011 Saudi International Electronics, Communications and Photonics Conference, Riyadh, Saudi Arabia, 24–26 April 2011; pp. 1–5. [CrossRef]
6. Sheng, Y.; Dun, X.; Jin, W.; Zhou, F.; Wang, X.; Mi, F.; Xiao, S. The On-Orbit Non-Uniformity Correction Method with Modulated Internal Calibration Sources for Infrared Remote Sensing Systems. *Remote Sens.* **2018**, *10*, 830. [CrossRef]
7. Lee, S.Y.; Kim, G.H.; Lee, Y.S.; Kim, G.S. Thermal performance analysis of vacuum variable-temperature black-body system. *Infrared Phys. Technol.* **2014**, *64*, 97–102. [CrossRef]

8.   Miao, L.F.; Xu, Q.; Zhang, M.T.; Sun, D.X.; Liu, Y.N. Real-time implementation of multi-point non-uniformity correction for IRFPA based on FPGA. In *International Symposium on Photoelectronic Detection and Imaging 2009: Advances in Infrared Imaging and Applications*; International Society for Optics and Photonics: Bellingham, WA, USA, 2009; Volume 7383, pp. 1–8.

9.   Song, S.; Zhai, X. Research on non-uniformity correction based on blackbody calibration. In Proceedings of the 2020 IEEE 4th Information Technology, Networking, Electronic and Automation Control Conference (ITNEC), Chongqing, China, 12–14 June 2020; Volume 1, pp. 2146–2150. [CrossRef]

10.   Morozova, S.P.; Sapritsky, V.I.; Ivanov, V.S.; Lisiansky, B.E.; Melenevsky, U.A.; Xi, L.Y.; Pei, L. Facility for blackbody calibration. In Proceedings of the 7th International Symposium on Temperature and Thermal Measurements in Industry and Science, Delft, The Netherlands, 1–3 June 1999; pp. 587–592.

11.   Theocharous, E.; Fox, N.P.; I Sapritsky, V.; Mekhontsev, S.N.; Morozova, S.P. Absolute measurements of black-body emitted radiance. *Metrologia* **1998**, *35*, 549–554. [CrossRef]

12.   Sapritsky, V.I.; Khlevnoy, B.B.; Khromchenko, V.B.; Lisiansky, B.E.; Mekhontsev, S.N.; Melenevsky, U.A.; Morozova, S.P.; Prokhorov, A.V.; Samoilov, L.N.; Shapoval, V.I.; et al. Precision blackbody sources for radiometric standards. *Appl. Opt.* **1997**, *36*, 5403–5408. [CrossRef] [PubMed]

13.   Mason, I.M.; Sheather, P.H.; Bowles, J.A.; Davies, G. Blackbody calibration sources of high accuracy for a space-borne infrared instrument: The Along Track Scanning Radiometer. *Appl. Opt.* **1996**, *35*, 629–639. [CrossRef] [PubMed]

14.   Olschewski, F.; Ebersoldt, A.; Friedl-Vallon, F.; Gutschwager, B.; Hollandt, J.; Kleinert, A.; Monte, C.; Piesch, C.; Preusse, P.; Rolf, C.; et al. The in-flight blackbody calibration system for the GLORIA interferometer on board an airborne research platform. *Atmos. Meas. Tech.* **2013**, *6*, 3067–3082. [CrossRef]

15.   Monte, C.; Gutschwager, B.; Adibekyan, A.; Kehrt, M.; Ebersoldt, A.; Olschewski, F.; Hollandt, J. Radiometric calibration of the in-flight blackbody calibration system of the GLORIA interferometer. *Atmos. Meas. Tech.* **2014**, *7*, 13–27. [CrossRef]

16.   Xiong, X.; Chiang, K.; Esposito, J.; Guenther, B.; Barnes, W. MODIS on-orbit calibration and characterization. *Metrologia* **2003**, *40*, S89–S92. [CrossRef]

17.   Xiong, X.; Barnes, W. An overview of MODIS radiometric calibration and characterization. *Adv. Atmos. Sci.* **2006**, *23*, 69–79. [CrossRef]

18.   Oh, H.-U.; Shin, S. Numerical study on the thermal design of on-board blackbody. *Aerosp. Sci. Technol.* **2012**, *18*, 25–34. [CrossRef]

19.   Oh, H.-U.; Shin, S.; Kim, J.-M. On-Orbit Performance Prediction of Black Body Based on Functional Test Results under Ambient Condition. *J. Aerosp. Eng.* **2012**, *25*, 39–44. [CrossRef]

20.   Oh, H.-U.; Lee, M.-J.; Kim, T. Experimental Design Validation of Tilting Calibration Mechanism by Using Shape Memory Alloy Spring Actuator. *Int. J. Aerosp. Eng.* **2017**, *2017*, 1–12. [CrossRef]

21.   *Thermal Desktop User's Guide, Ver. 6.1*; Network Analysis Associates: Tempe, AZ, USA, 2006.

22.   *SINDA/FLUINT User's Guide, Ver. 6.1*; Network Analysis Associates: Tempe, AZ, USA, 2006.